Regular Article

PHYSICAL CHEMISTRY RESEARCH
Published by the
Iranian Chemical Society
www.physchemres.org
info@physchemres.org

Phys. Chem. Res., Vol. 9, No. 2, 227-239, June 2021
DOI: 10.22036/pcr.2021.243284.1804

A Facile Protocol for Designing the CdS/PbS Multi Layered Quantum Dots with Enhanced Photoelectrochemical Performance

S. Sadeghi, M. Jafarian* and G.S. Ferdowsi

Department of Chemistry, K.N. Toosi University of Technology, P. O. Box: 15875-4416, Tehran, Iran

(Received 10 August 2020, Accepted 9 January 2021)

Photocatalysts play a vital role in solar cell performances; solar cells are an effective source of green energy. In this paper, a facile and affordable protocol for designing an effective photoanode based on the quantum dot was introduced. The multi-layered quantum dots containing CdS and different layers of n-type of PbS (2, 4, 6 cycles) have been used to improve photoanodes sensitivity through the successive ionic layer adsorption and reaction (SILAR) with a coat of TiO_2 nanoparticles on the ITO substrates. CuS was used as a counter electrode for all cells. The film's behavior was examined in the darkness and under simulated sunlight (200 mW cm^{-2}) with electrochemical techniques including chronoamperometry, chronopotentiometry, electrochemical impedance spectroscopy and linear sweep voltammetry. The morphology of the prepared films was investigated by scanning electron microscopy and energy dispersive X-Ray spectroscopy. The results for the TiO_2/4CdS/4PbS film revealed that developing multi-layered cells could improve the quantum dot sensitivity and the performance of the cell in case of reaching the optical layer. The TiO_2/4CdS/4PbS electrode improved the sensitivity of the cell remarkably and the maximum difference between light and darkness was observed in the potential of 1.5 V, in which the constant potential current of 1.5 V led to the cm^2 difference in chronoamperometry by 18 µA cm^{-2}.

Keywords: SILAR, Semiconductors, Photoelectrochemical, CdS, PbS

INTRODUCTION

In recent years, photocatalyst has attracted much attention, due to the ability to convert solar energy to electrical energy as well as other diverse applications [1]. Since semiconductors such as ZnO, TiO_2 require ultraviolet light for photocatalytic performance due to their wide bandgaps, finding and designing photocatalysts that can work under visible light is a hot topic. Although CdS is a promising photocatalyst due to the high absorption of visible light and its proper bandgap, two factors, the high recombination of electron and hole couples generated by photo and intensely photo corrosion in pristine CdS, limit the use of this promising substance. To resolve this problem, researchers have introduced composites and heterojunction photocatalysts like graphene/CdS [2-4], CdS/CdSe/ZnS [5] CdS/CdTeS [6], Au,Ag/CdS [7,8], TiO_2/CdS [9,10] MoS_2/CdS [11,12] and other composites based on CdS [13-15]. CdS-based composites have a high photocatalytic activity, especially in the presence of noble metals that, due to high costs, have no industrial application. Therefore, the development of affordable photocatalysts has been of much interest [16]. Lead sulfide (PbS) is an important semiconductor with a narrow bandgap (0.37-0.41 eV) [17-21]. In PbS, an excited electron jumps from the valence band to the conductive band during the light exposure, forming a hole in the valence band. So the electron-hole movement in the lattice structure brings the conductivity properties for PbS. This feature of PbS has drawn much interest from researchers. As studies show, PbS can couple with CdS and the epitaxial growth of PbS on single CdS crystals improves the performance of the cell [22,23]. Changing the stoichiometric parameters of sulfur in the lattice structure of PbS can impart different sorts of PbS

*Corresponding author. E-mail: mjafarian@kntu.ac.ir

semiconductors including the n-type and the p-type, which are the results of a decrease and an increase in the stoichiometric parameters of sulfur, respectively [24,25]. Likewise, in recent years, semiconductors of quantum dots (QDs) have attracted attention because of their unique properties [26]. There are various QDs which can be used in solar cells [27-39].

Lots of methods have been employed in developing the thin-film and quantum dot cells such as chemical bath deposition (CBD), electrodeposition (ED), successive ionic layer adsorption and reaction (SILAR) [17]. Use of successive ionic layer adsorption and reaction (SILAR) process for absorption semiconductors such as CdS, PbS, CdSe, *etc.* is an affordable and facile method for coating the wide-gap semiconductors like TiO_2 with a low thickness [18]. Increasing SILAR cycles can also lead to layers with different thicknesses and large particles [19]. This method can improve the performance of the cell at the optical layer [20], since the electron from the radiation of Ti^{3+} (in TiO_2 substrate) would be trapped as a result of increasing the number of SILAR cycles, slowing down the kinetics. In this work, 4 layers of CdS and different layers of PbS have been grown on TiO_2 film substrate on ITO glass using the SILAR method to create the photoanode electrode.

EXPERIMENTAL

Materials and Methods

All the chemical materials used in this work were in analytical grade (Merck) and all electrochemical measurements were carried out by the Potentiostat/ Galvanostat device (Eg&G, model 273A) controlled by a PC through M270 and M398 software (GPIB interface). Electrochemical Impedance Spectroscopy device (Solartron, model SI 1255) was used to measure the electrochemical properties of the cells in darkness and under simulated sunlight (200 mW cm^{-2}) conditions. The surface morphology of the working electrode was investigated by field emission scanning electron microscopy (FESEM), model SIGMA VP (ZEISS company of Germany), also the energy dispersive X-ray spectroscopy (EDS) and mapping detector was made by Oxford Instrument company of England. X-ray diffraction (XRD) study was performed by X-ray diffractometer model, X' Pert Pro (Panalytical company). All experiments were performed at temperature of 25 °C.

Preparation of TiO_2

TiO_2 paste was prepared by mixing 3 g of titanium dioxide powder with a few drops of diluted acetic acid. To make pores in the TiO_2 paste, 0.5 g of carboxymethyl cellulose (CMC) was mixed with 2 ml of ethanol in another beaker. After mixing for 15 min, these two solutions were mixed and stirred with a magnetic stirrer for 1 hr at 50 °C to remove ethanol and water. Finally, a few drops of paraffin was added to increase the adhesiveness and viscosity of the TiO_2 paste. After cooling off, the TiO_2 paste was coated with indium tin oxide glass (ITO) sheet with the resistance of (20-30 Ω/sq) using the doctor blading method and then annealed at 350 °C for 1 h. To minimize cracking, the glass should be heated at a slow pace. To make the photoanode, TiO_2 film glass was coated with CdS and PbS, respectively, using successive ionic layer adsorption and reaction (SILAR) method. The size of sensitized electrodes (photoanode and photocathode) was 1 × cm^{-2}.

Preparation of Photoanodes

$Cd(NO_3)_2$ (0.1 M) and Na_2S (0.1 M) were used as precursors to fabricate the CdS layer. The TiO_2 film was dip-coated into the $Cd(NO_3)_2$ solution for 1 s and subsequently into Na_2S for 1 s. At last, the electrode was rinsed with distilled water to remove unadsorbed particles, then dried with a dryer. This procedure was repeated for four times to fabricate 4 layers of CdS on the TiO_2 film. To improve the sensitivity of photoanode, different layers of n-type PbS semiconductor was grown on the CdS film. $Pb(NO_3)_2$ (0.1 M) and Na_2S (0.1 M) were used as precursors. PbS film was coated on CdS by dipping CdS film alternately into the $Pb(NO_3)_2$ and Na_2S for 1s (SILAR method) and then rinsed with distilled water, this was repeated to create different numbers of SILAR cycles such as 2, 4 and 6 to obtain the different thicknesses of TiO_2/4CdS/nPbS layers.

Preparation of Photocathodes

SILAR deposition of CuS onto the ITO glass was performed to prepare CEs. $CuSO_4$ (0.1 M) and Na_2S (0.1 M) were used as precursors. ITO glass was then immersed in

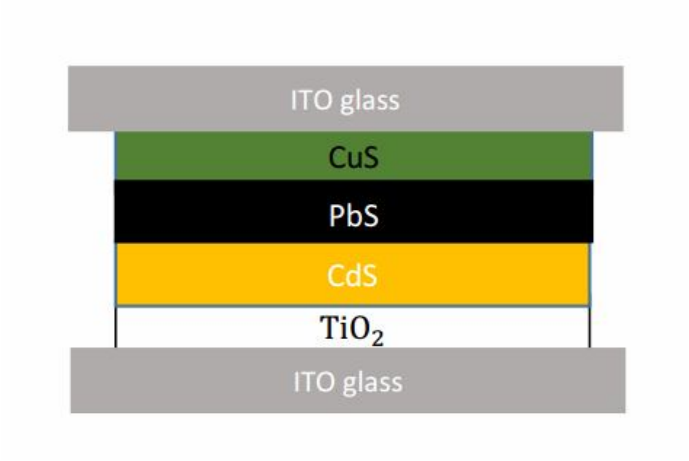

Fig. 1. Schematic structure of the prepared cell.

the $CuSO_4$ solution for 1 min and then dipped in the Na_2S solution for another 1 min. Then, the counter electrode was rinsed with distilled water and dried with a dryer. This operation was repeated for four times to make the 4CuS layers.

Assembling the Cell

At last, the two coated glass sides were attached by binder clips where the layer of TiO_2/4CdS/nPbS was the photoanode and CuS was the photocathode (Fig. 1). It should be noted that no electrolyte was injected into the cell.

RESULTS AND DISCUSSION

Structure of the Prepared Electrode

Figure 2 shows the SEM images of a mesoporous TiO_2 layer onto the ITO glass prepared in the experimental section. According to this figure, the TiO_2 layer contains 16-43 nm particles. X-ray diffraction (XRD) technique was used for further study of the structure and the physical properties of the TiO_2 film. As shown in Fig. 3, the XRD pattern demonstrated the presence of anatase phase of TiO_2. The Scherrer equation was used to calculate the average size of the TiO_2 crystal Eq. (1). In this equation, D is the size of the crystals, γ is the X-ray wavelength (0.154 nm), β is the line broadening at half the maximum intensity (FWHM) and θ is the Bragg angle.

$$D = \frac{0.9\gamma}{\beta \cos\theta} \quad (1)$$

The crystal size measured by the Scherrer equation was about 50 nm, which confirmed the nanocrystalline size of the TiO_2 film. As already mentioned, the CdS film was sensitized by different layers of n-type PbS using the SILAR cycles to improve efficiency.

The elemental analysis of the TiO_2/4CdS/4PbS film is shown in Fig. 4. This spectrum reveals the presence of C, O, S, Ti, Cd, Sn and Pb elements with atomic percentage of 7.55%, 9.33%, 24.78%, 7.31%, 6.68%, 4.03% and 40.32%, respectively. The percentages prove the presence of PbS over the surface of the TiO_2/4CdS film. Due to the combination of PbS shown in Fig. 4, decrease of sulfur content in the lattice structure leads to the formation of n-type PbS semiconductor. As a result, n-type PbS can improve the sensitivity of the CdS film.

Photocurrent-voltage Characteristics

The photocurrent density graph with applied potential (I-V) in dark and under simulated sunlight (200 mW cm^{-2}) for different layers of PbS is shown in Fig. 5. Linear sweep voltammetry (LSV) was carried out at the scan rate of 100 (mV s^{-1}) in the potential range of -0.3 V to 1.5 V. As illustrated in Fig. 5a, the cell with the lowest current and sensitivity to light and darkness was the TiO_2/4CdS/6PbS film, which seems to be the result of the increasing size of the quantum dot particles. Similarly, the TiO_2 layer which was slightly coated with CdS and PbS showed less sensitivity to darkness and light in the TiO_2/4CdS/2PbS electrode. In the fourth layer of PbS (TiO_2/4CdS/4PbS

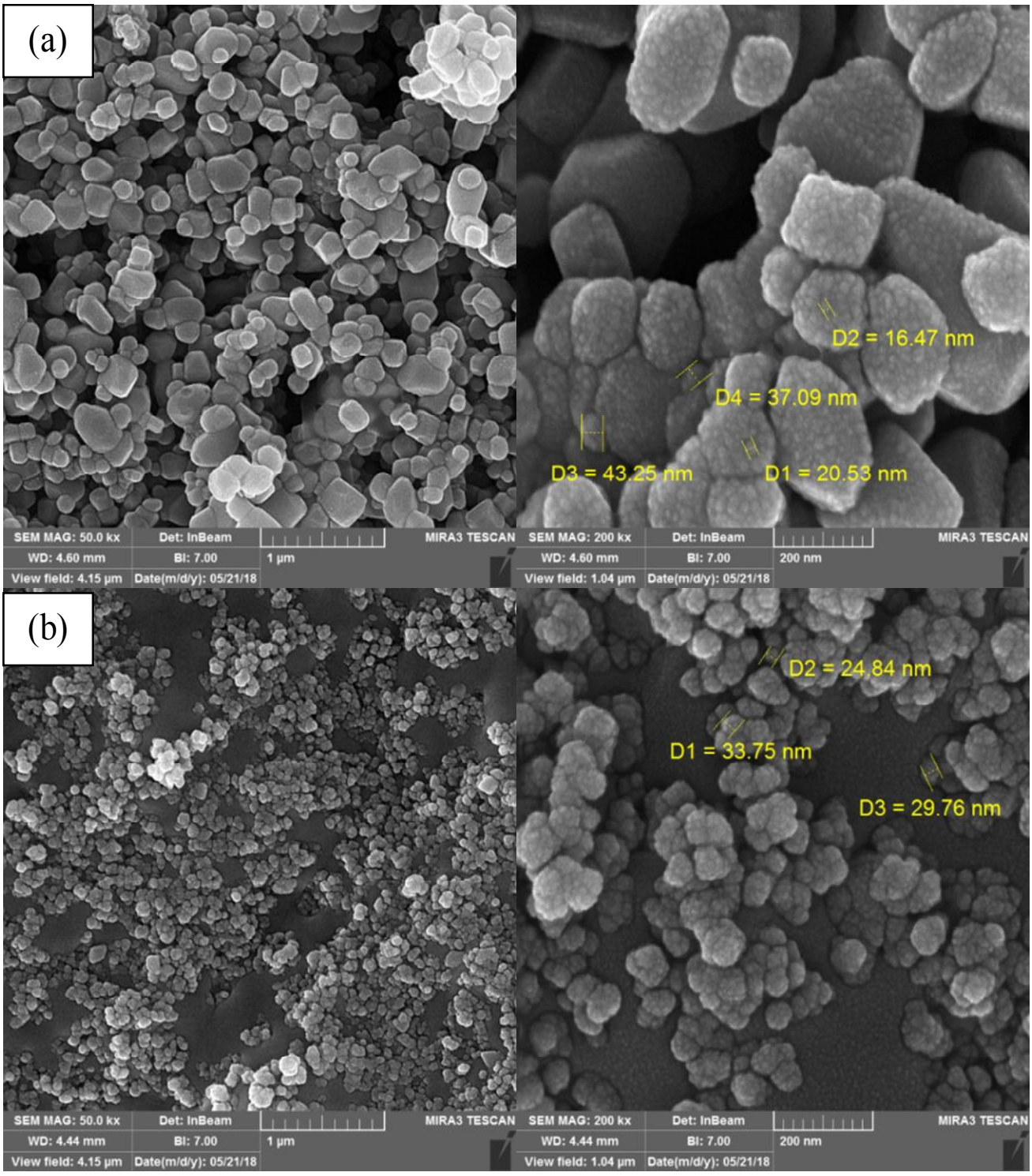

Fig. 2. SEM images of (a) TiO_2 nanoparticles and (b) TiO_2/4CdS/4PbS electrode.

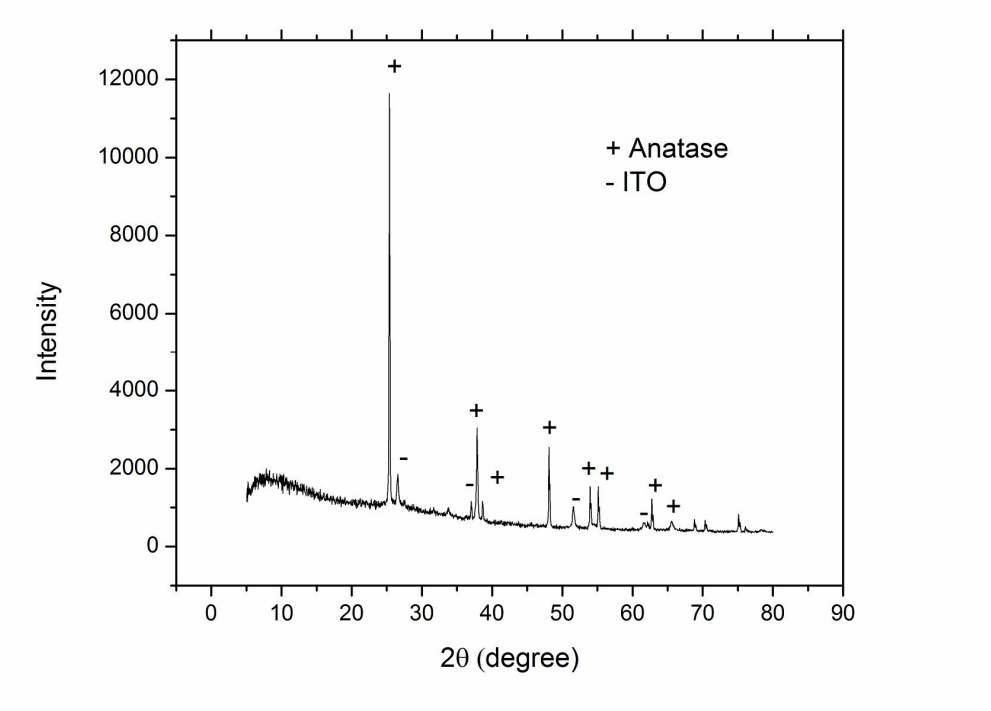

Fig. 3. The XRD spectrum of TiO_2 paste onto the ITO substrate.

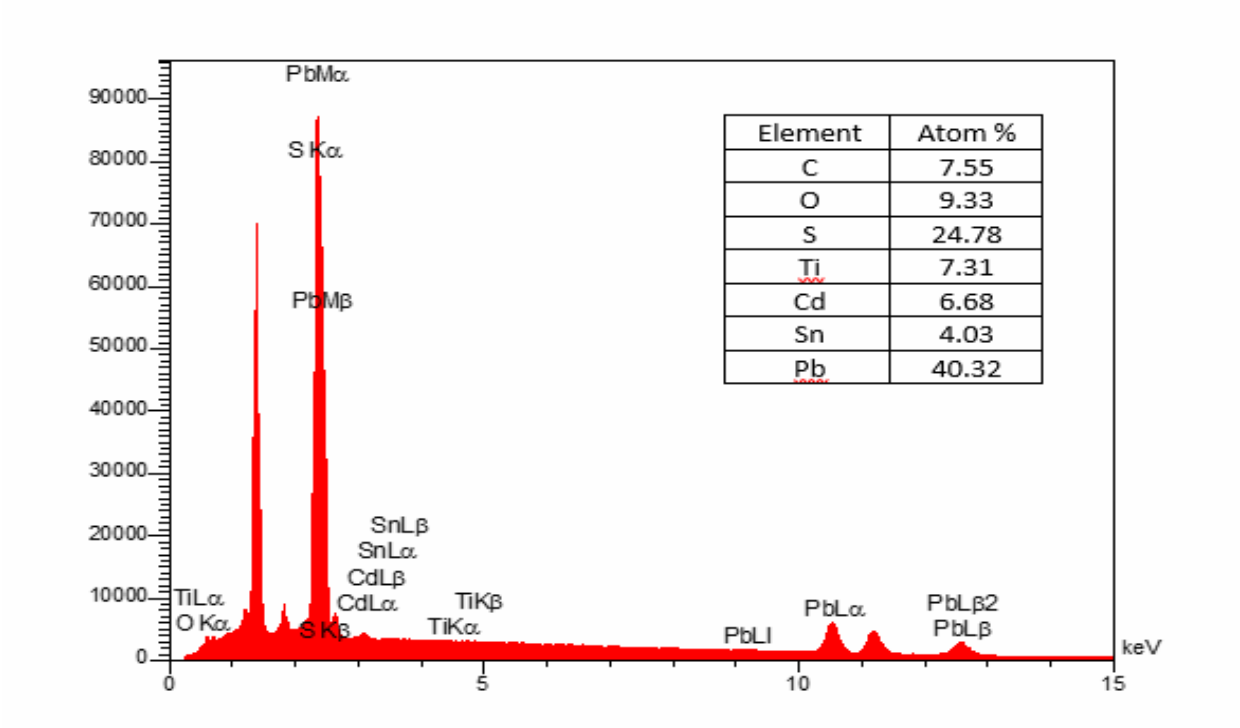

Element	Atom %
C	7.55
O	9.33
S	24.78
Ti	7.31
Cd	6.68
Sn	4.03
Pb	40.32

Fig. 4. EDS of TiO_2/4CdS/4PbS film with atomic percentage.

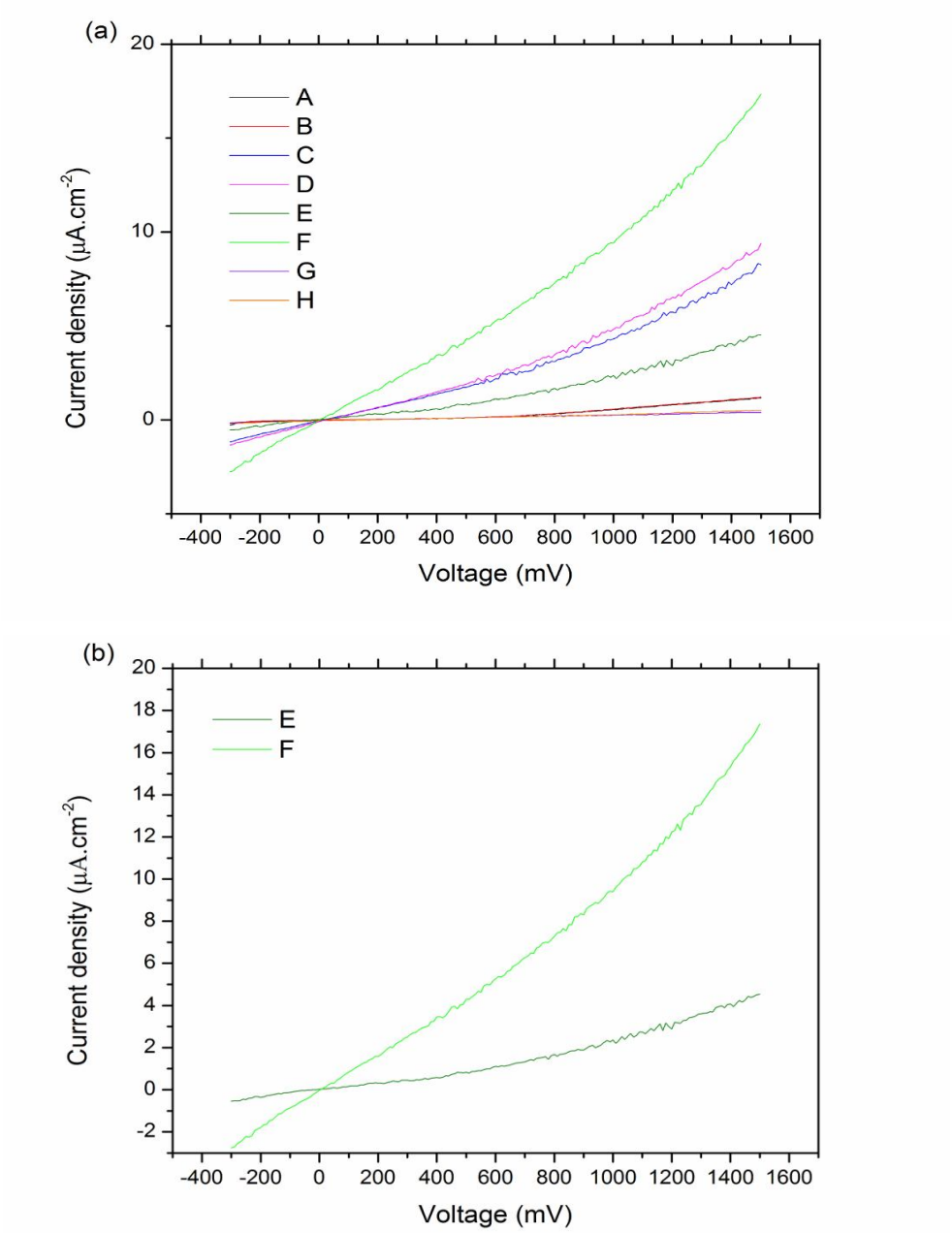

Fig. 5. The I-V curves for (a) different layers of PbS A-TiO_2/4CdS/0PbS in dark, B-TiO_2/4CdS/0PbS in light, C-TiO_2/4CdS/2PbS in dark, D-TiO_2/4CdS/2PbS in light, E-TiO_2/4CdS/4PbS in dark, F-TiO_2/4CdS/4PbS in light, G-4CdS/6PbS in dark, and H-TiO_2/4CdS/6PbS in light conditions.(b) TiO_2/4CdS/4PbS electrode in E-Dark, and F-Light conditions.

film), due to the suitable cover of TiO_2 with CdS and PbS, sensitivity and current density were increased. These results indicated that the number of coated layers on the TiO_2 film has a vital role in the efficiency and sensitivity of the cells. According to the LSV graph (linear sweep voltammetry) in Fig. 5b, the maximum difference between light and

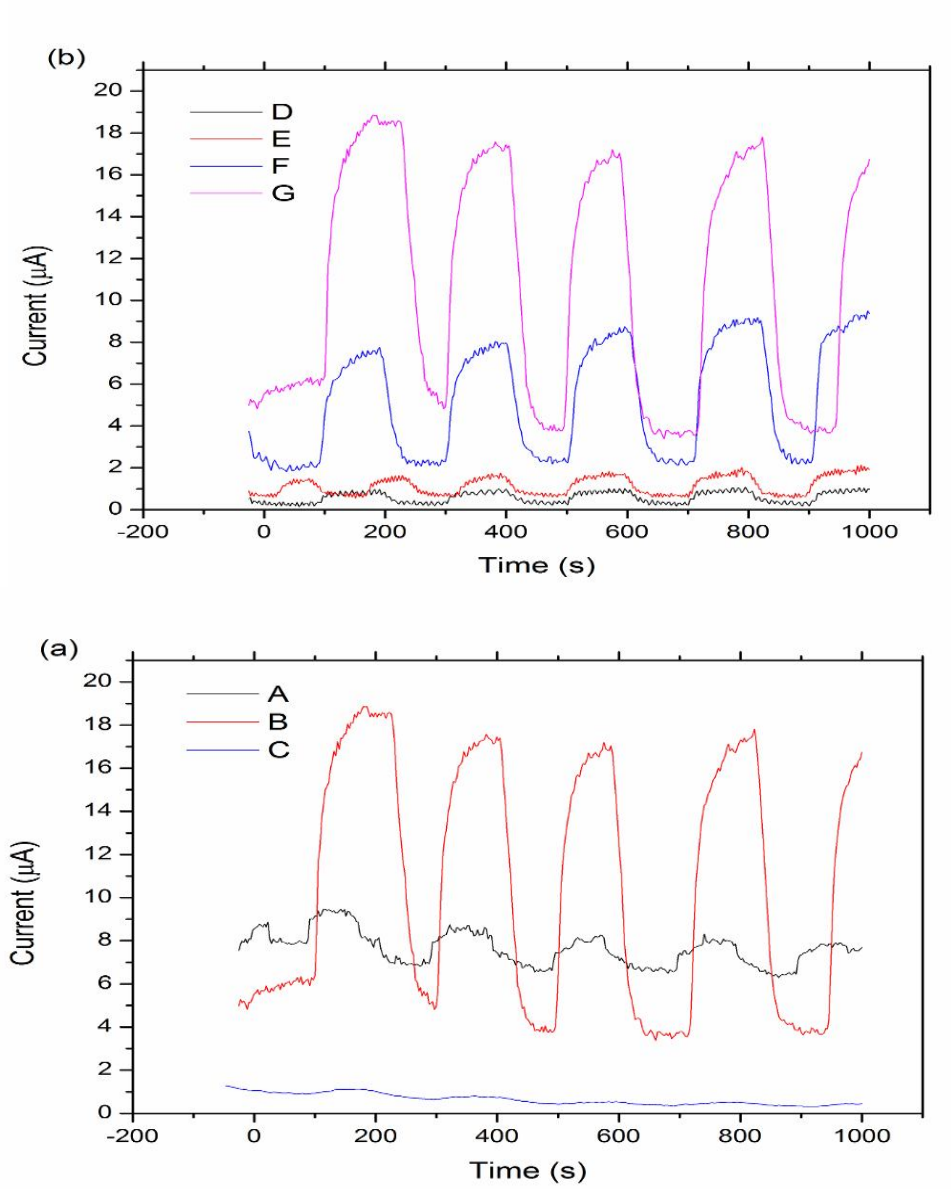

Fig. 6. Photocurrent under 100s light and 100s dark conditions for (a) different layers of PbS, A-TiO_2/ 4CdS/2PbS, B-TiO_2/4CdS/4PbS, and C-TiO_2/4CdS/6PbS. (b) TiO_2/4CdS/4PbS electrode by applied different potentials of D-0.2 V, E- 0.5 V, F-1 V, G-1.5 V.

darkness was observed in the potential of 1.5 V which reached about 13 μA, with CA (chronoamperometry) delivering the same results as well.

Photoresponse and Photostability of the Prepared Cells

The photoresponse of TiO_2/4CdS/nPbS film was measured by chronoamperometry (CA) and chronopotentiometry (CE) techniques. Film's behavior was measured in darkness and under chopped light (light on 100s, light off 100s). As shown in Fig. 6a, the TiO_2/4CdS /4PbS cell was more sensitive than TiO_2/4CdS/2PbS, and TiO_2/4CdS/6PbS had the highest photocurrent and was so photoresponsive. Therefore, TiO_2/4CdS/4PbS was

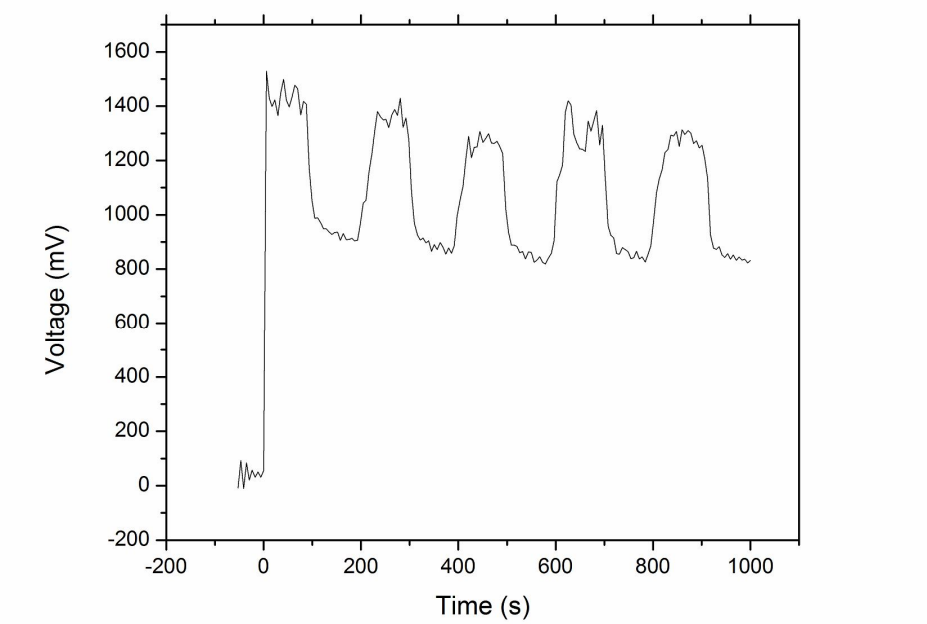

Fig. 7. V-t response of the TiO_2/4CdS/4PbS cell under 100s light and 100s dark conditions for1000s.

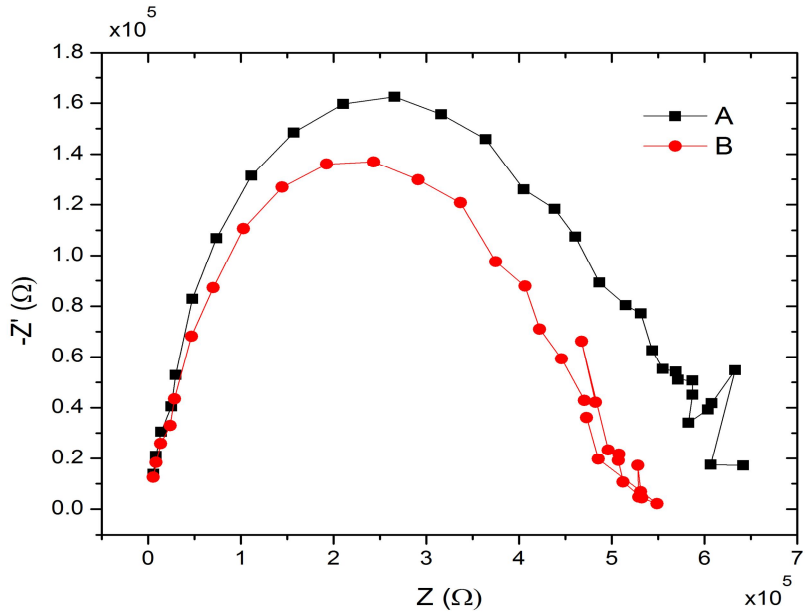

Fig. 8. Nyquist plots for TiO_2/4CdS/4PbS electrode under A-dark condition, and B-light illumination.

considered as the optical layer of photoanodes. For further investigation of TiO_2/4CdS/4PbS cell, chronoamperometry was applied at constant four potentials of 0.2, 0.5, 1, 1.5 V (Fig. 6b). The current for TiO_2/4CdS/4PbS electrode rises to the maximum immediately after turning the light on and it almost remained unchanged. The light was turned off

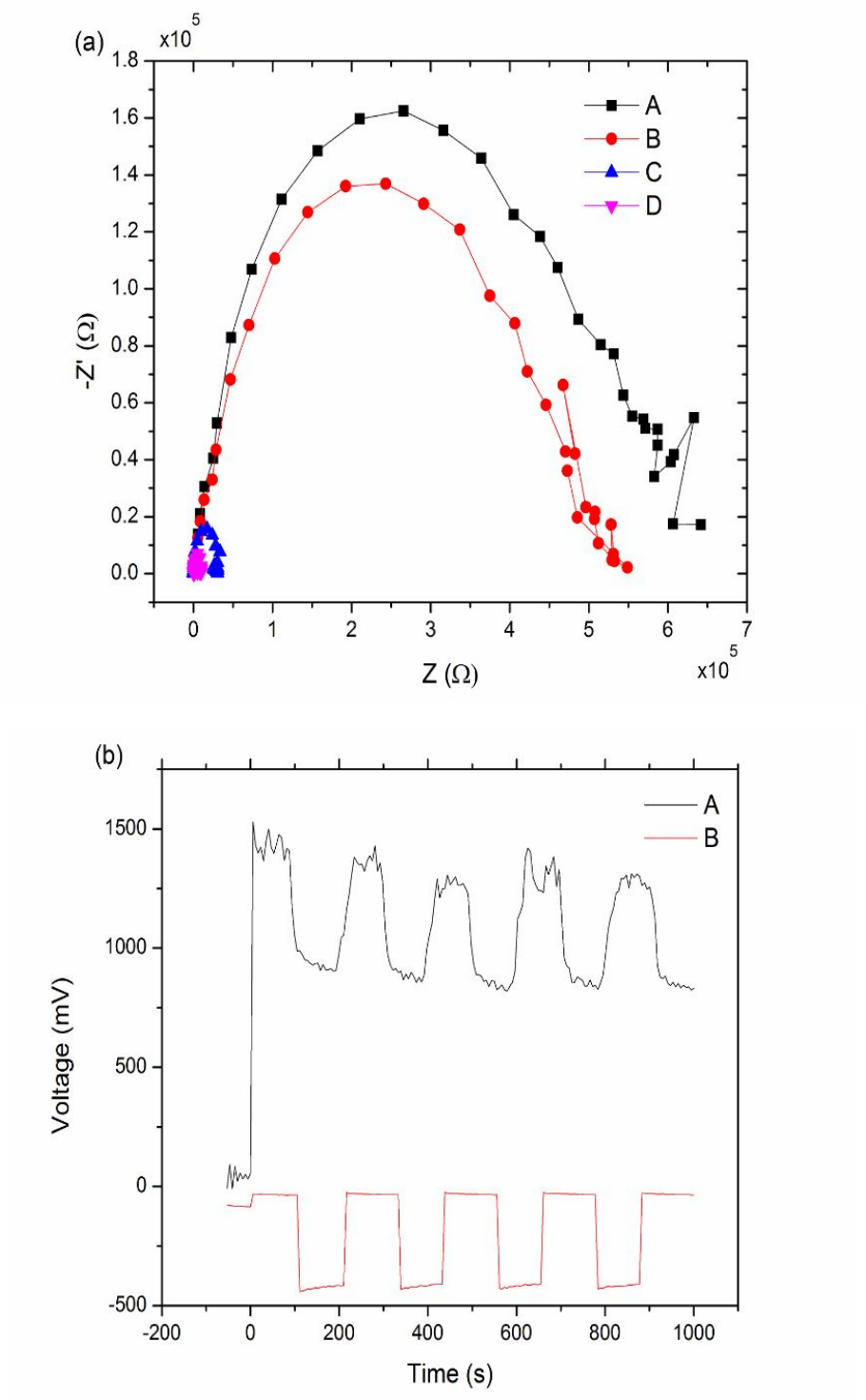

Fig. 9. (a) Nyquist plots for A-TiO_2/4CdS/4PbS cell under dark condition, B-TiO_2/4CdS/4PbS cell under light illumination, C-industrial cell under dark condition, and D-industrial cell under light illumination. (b)V-t response under light and darkness of A-TiO_2/4CdS/4PbS cell, and B-industrial cell for 1000s.

after 100s and the photocurrent of the TiO_2/4CdS/4PbS film decreased instantly to the nearly dark current. This was repeated for 1000s and the result showed that the TiO_2/4CdS/4PbS cell has the proper stability and fast photoresponse.

The photovoltage of the TiO_2/4CdS/4PbS film was measured by the chronopotentiometry technique, under simulated sunlight irradiation (200 mW cm^{-2}) (100s dark and 100s light), in 10 μA for 1000s. As shown in Fig. 7, the TiO_2/4CdS/4PbS film can reach the potential of 1400 mV potential under visible light illumination. As the generation of an electron in photoanode (TiO_2/4CdS/4PbS) and the recombination of the hole in photocathode (CuS) are done to the same extent, the cell reaches a dynamic equilibrium. So, it is expected that the electrode is shifted to the same extent (positively and negatively) whether the light is on or off.

EIS Characteristics

The Nyquist spectra of the TiO_2/4CdS/4PbS cell under dark and light conditions are shown in Fig. 8, frequency was scanned from 100 KHz to 100 mHz (DC potential of 1 V and AC potential of 15 mV). As illustrated, the beginning and charge-transfer resistance (Rct) decreased from 47.58 kOhm, and 531.3 kOhm to 46.79 kOhm, and 496.2 kOhm under light illumination. The beginning resistance in the charts reveals that the cell has become more conductive under illumination, and the charge transfer resistance shows that the electron mobility is improved and the kinetics are fast.

Comparison the Prepared Cell with an Industrial Cell

For further review, the TiO_2/4CdS/4PbS cell was compared with a silicon industrial cell using chronopotentiometry and applying the current of 10 μA and also using the EIS method with previous conditions. As shown in Fig. 9a, under illumination, the charge transfer resistance was about 1.379 kOhm and the beginning resistance was 16.64 Ohm. In the darkness, the charge transfer resistance and the beginning resistance were 26.78 and 16.91 Ohm, respectively. These values of resistance are very low compared to the TiO_2/4CdS/4PbS cell. According to Ohm's law, increasing the resistance would increase the potential Fig. 9b. Thus, the low current density produced by the TiO_2/4CdS/4PbS electrode is the result of the high resistances, however, the photoresponse of both cells to darkness and light was the same as Fig. 9b.

CONCLUSIONS

In this study, TiO_2/4CdS/nPbS quantum dot photoanodes were developed by SILAR method to improve the performance of anode in photocell. According to the experimental studies, TiO_2/4CdS/4PbS had the best performance. The TiO_2/4CdS/4PbS electrode improved the sensitivity of the cell remarkably and the maximum difference between light and darkness was observed in the potential of 1.5 V, in which the constant potential current of 1.5 V led to the difference in chronoamperometry by 18 μA cm^{-2}. In fact, the sensitivity and photoresponse of the TiO_2 film were improved by using sensitized multi-layered quantum dots while reaching the optical layer of PbS. It should be noted that these results were confirmed by the electrochemical impedance spectroscopy technique.

ACKNOWLEDGEMENTS

The financial support of this research provided by K.N. Toosi University of Technology research council.

Conflict of Interest

The authors declare that they have no conflict of interest.

REFERENCES

[1] Wang, R.; Chen, S.; Ng, Y. H.; Gao, Q.; Yang, S.; Zhang, S.; Peng, F.; Fang, Y.; Zhang, S., ZnO/CdS/PbS Nanotube arrays with multi-heterojunctions for efficient visible-light-driven photoelectrochemical hydrogen evolution. *Chem. Eng. J.* **2019**, *362*, 658-666, DOI: 10.1016/j.cej.2019.01.073.

[2] Singh, A.; Sinha, A. S. K., Active CdS/RGO photocatalyst by a high temperature gas-solid reaction for hydrogen production by splitting of water. *Appl. Surf. Sci.* **2018**, *430*, 184-197, DOI: 10.1016/

j.apsusc.2017.02.214.

[3] Zhu, Z.; Han, Y.; Chen, C.; Ding, Z.; Long, J.; Hou, Y., Reduced graphene oxide-cadmium sulfide nanorods decorated with silver nanoparticles for efficient photocatalytic reduction carbon dioxide under visible light. *Chem. Cat. Chem* **2018**, *10*, 1627-1634, DOI: 10.1002/cctc.201701573.

[4] Han, W.; Chen, L.; Song, W.; Wang, S.; Fan, X.; Li, Y.; Zhang, F.; Zhang, G.; Peng, W., Synthesis of nitrogen and sulfur Co-doped reduced graphene oxide as efficient metal-free cocatalyst for the photo-activity enhancement of CdS. *Appl. Catal. B Environ* **2018**, *236*, 212-221.

[5] Cheng, S.; Fu, W.; Yang, H.; Zhang, L.; Ma, J.; Zhao, H.; Sun, M.; Yang, L., Photoelectrochemical performance of multiple semiconductors (CdS/CdSe/ZnS) cosensitized TiO_2 photoelectrodes. *J. Phys. Chem. C* **2012**, *116*, 2615-2621, DOI: 10.1016/j.apcatb.2018.05.021.

[6] Tang, Z.; Wang, Y.; Shanbhag, S.; Kotov, N. A., Spontaneous CdTe → Alloy → CdS transition of stabilizer-depleted CdTe nanoparticles induced by EDTA. *J. Am. Chem. Soc*. **2006**, *128*, 7036-7042, DOI: 10.1021/ja055366w.

[7] Kumar, N.; Komarala, V. K.; Dutta, V., *In-situ* synthesis of Au-CdS plasmonic photocatalyst by continuous spray pyrolysis and its visible light photocatalysis. *Chem. Eng. J.* **2014**, *236*, 66-74, DOI: 10.1016/j.cej.2013.09.052.

[8] Liu, Y.; Chi, M.; Dong, H.; Jia, H.; Xu, B.; Zhang, Z., Ag/CdS Heterostructural composites: Fabrication, characterizations and photocatalysis. *Appl. Surf. Sci.* **2014**, *313*, 558-562, DOI: 10.1016/j.apsusc.2014.06.022.

[9] Zhou, P.; Le, Z.; Xie, Y.; Fang, J.; Xu, J., Studies on facile synthesis and properties of mesoporous CdS/TiO_2 composite for photocatalysis applications. *J. Alloys Compd* **2017**, *692*, 170-177, DOI: 10.1016/j.jallcom.2016.09.039.

[10] Meng, A.; Zhu, B.; Zhong, B.; Zhang, L.; Cheng, B., Direct Z-Scheme TiO_2/CdS hierarchical photocatalyst for enhanced photocatalytic H_2-production activity. *Appl. Surf. Sci* **2017**, *422*, 518-527, DOI: 10.1016/j.apsusc.2017.06.028.

[11] Li, J.; Peng, Y.; Qian, X.; Lin, J., Few-layer Co-doped MoS_2 nanosheets with rich active sites as an efficient cocatalyst for photocatalytic H_2 production over CdS. *Appl. Surf. Sci.* **2018**, *452*, 437-442, DOI: 10.1016/j.apsusc.2018.05.021.

[12] Chai, B.; Xu, M.; Yan, J.; Ren, Z., Remarkably enhanced photocatalytic hydrogen evolution over MoS_2 nanosheets loaded on uniform CdS nanospheres. *Appl. Surf. Sci.* **2018**, *430*, 523-530, DOI: 10.1016/j.apsusc.2017.07.292.

[13] Pan, J.; Liu, J.; Zuo, S.; Khan, U. A.; Yu, Y.; Li, B., Structure of Z-Scheme CdS/CQDs/BiOCl heterojunction with enhanced photocatalytic activity for environmental pollutant elimination. *Appl. Surf. Sci*. **2018**, *444*, 177-186, DOI: 10.1016/j.apsusc.2018.01.189.

[14] Chai, Y. -Y.; Qu, D. -P.; Ma, D. -K.; Chen, W.; Huang, S., Carbon quantum dots/Zn^{2+} ions doped-CdS nanowires with enhanced photocatalytic activity for reduction of 4-nitroaniline to *p*-phenylenediamine. *Appl. Surf. Sci*. **2018**, *450*, 1-8, DOI: 10.1016/j.apsusc.2018.04.121.

[15] Fang, X.; Cui, L.; Pu, T.; Song, J.; Zhang, X. Core-shell CdS@MnS nanorods as highly efficient photocatalysts for visible light driven hydrogen evolution. *Appl. Surf. Sci*. **2018**, *457*, 863-869, DOI: 10.1016/j.apsusc.2018.07.012.

[16] Liu, Y.; Shen, S.; Zhang, J.; Zhong, W.; Huang, X., Cu^{2-} XSe/CdS composite photocatalyst with enhanced visible light photocatalysis activity. *Appl. Surf. Sci.* **2019**, *478*, 762-769, DOI: 10.1016/j.apsusc.2019.02.010.

[17] Al-Zuhery, A. M.; Al-Jawad, S. M.; Al-Mousoi, A. K., The effect of PbS thickness on the performance of CdS/PbS solar cell prepared by CSP. *Optik (Stuttg)* **2017**, *130*, 666-672, DOI: 10.1016/j.ijleo.2016.10.120.

[18] Jiménez-García, F. N.; Segura-Giraldo, B.; Restrepo-Parra, E.; López-López, G. A., Synthesis of TiO_2 thin films by the SILAR method and study of the influence of annealing on its structural, morphological and optical properties. *Ingeniare. Rev. Chil. Ing*. **2015**, *23*, 622-629. Deepa, K. G.; Nagaraju, J., Development of SnS quantum dot solar cells by SILAR method.

Mater. Sci. Semicond. Process **2014**, *27*, 649-653, DOI: 10.1016/ j.mssp.2014.08.006.

[19] Samadpour, M.; Arabzade, S., Graphene/CuS/PbS nanocomposite as an effective counter electrode for quantum dot sensitized solar Cells. *J. Alloys Compd.* **2017**, *696*, 369-375, DOI: 10.1016/ j.jallcom.2016.11.268.

[20] Heidaripour, A.; Jafarian, M.; Gobal, F.; Mahjani, M. G.; Miandari, S., Investigation of Pb/PbS a positive schottky junction formed on conductive glass in contact with alkaline solution. *J. Appl. Phys.* **2014**, *116*, 34906, DOI: 10.1063/1.4890338.

[21] Watanabe, S.; Mita, Y., Electrical properties of CdS・PbS heterojunctions. *Solid. State. Electron* **1972**, *15*, 5-10, DOI: 10.1016/0038-1101(72)90061-5.

[22] Hernández-Borja, J.; Vorobiev, Y. V; Ramírez-Bon, R., Thin film solar cells of CdS/PbS chemically deposited by an ammonia-free process. *Sol. Energy Mater. Sol. Cells* **2011**, *95*, 1882-1888, DOI: 10.1016/ j.solmat.2011.02.012.

[23] Miandari, S.; Jafarian, M.; Mahjani, M. G.; Heidaripour, A., Photo-electrochemical studies by AC impedance spectroscopy on electrodeposited n-type PbS. *Bull. Chem. Soc. Jpn* **2014**, *88*, 209-216, DOI: 10.1246/bcsj.20140257.

[24] Joshi, R. K.; Durai, L.; Sehgal, H. K., Change of majority carrier type in PbS nanoparticle films. Phys. E low-dimensional syst. *Nanostructures* **2005**, *25*, 374-377, DOI: 10.1016/j.physe.2004.07.001.

[25] Shi, B.; Qi, Y.; Tian, L.; Liu, L., The enhanced photoelectrochemical performance of PbS/ZnS quantum dots Co-sensitized CdSe nanorods array heterostructure. *Mater. Sci. Semicond. Process* **2019**, *98*, 7-12, DOI: 10.1016/j.mssp.2019.03.018.

[26] Zhang, X.; Liu, J.; Zhang, J.; Vlachopoulos, N.; Johansson, E. M. J., ZnO@Ag_2S Core-shell nanowire arrays for environmentally friendly solid-state quantum dot-sensitized solar cells with panchromatic light capture and enhanced electron collection. *Phys. Chem. Chem. Phys.* **2015**, *17*, 12786-12795, DOI: 10.1039/C4CP06068G.

[27] Han, M.; Jia, J.; Yu, L.; Yi, G., Fabrication and photoelectrochemical characteristics of $CuInS_2$ and PbS quantum dot Co-sensitized TiO_2 nanorod photoelectrodes. *Rsc. Adv.* **2015**, *5*, 51493-51500, DOI: 10.1039/C5RA07409F.

[28] Guo, E.; Yin, L.; Zhang, L., CdS quantum dot sensitized anatase TiO_2 hierarchical nanostructures for photovoltaic application. *Cryst. Eng. Comm.* **2014**, *16*, 3403-3413, DOI: 10.1039/C4CE00019F.

[29] Larsen, G. K.; Fitzmorris, B. C.; Longo, C.; Zhang, J. Z.; Zhao, Y., Nanostructured homogenous CdSe-TiO_2 composite visible light photoanodes fabricated by oblique angle codeposition. *J. Mater. Chem.* **2012**, *22*, 14205-14218, DOI: 10.1039/C2JM32551A.

[30] Thulasi-Varma, C. V.; Rao, S. S.; Ikkurthi, K. D.; Kim, S. -K.; Kang, T. -S.; Kim, H. -J., Enhanced photovoltaic performance and morphological control of the PbS counter electrode grown on functionalized self-assembled nanocrystals for quantum-dot sensitized solar cells *via* cost-effective chemical bath deposition. *J. Mater. Chem. C* **2015**, *3*, 10195-10206, DOI: 10.1039/C5TC01988E.

[31] Kuo, C. -Y.; Su, M. -S.; Ku, C. -S.; Wang, S. -M.; Lee, H. -Y.; Wei, K. -H., Ligands affect the crystal structure and photovoltaic performance of thin films of PbSe quantum dots. *J. Mater. Chem* **2011**, *21*, 11605-11612, DOI: 10.1039/C0JM04417B.

[32] Kim, D. -H.; Lee, S. -J.; Park, M. S.; Kang, J. -K.; Heo, J. H.; Im, S. H.; Sung, S. -J., Highly reproducible planar Sb_2S 3-sensitized solar cells based on atomic layer deposition. *Nanoscale* **2014**, *6*, 14549-14554, DOI: 10.1039/C4NR04148H.

[33] Yan, S.; Zhang, L.; Tang, Y.; Lv, Y., Synthesis of water-soluble Ag_2Se QDs as a novel resonance rayleigh scattering sensor for highly sensitive and selective ConA detection. *Analyst* **2014**, *139*, 4210-4215, DOI: 10.1039/C4AN00579A.

[34] Chibli, H.; Carlini, L.; Park, S.; Dimitrijevic, N. M.; Nadeau, J. L., Cytotoxicity of InP/ZnS quantum dots related to reactive oxygen species generation. *Nanoscale* **2011**, *3*, 2552-2559, DOI: 10.1039/ C1NR10131E.

[35] Kan, S.; Aharoni, A.; Mokari, T.; Banin, U., Shape control of III-V semiconductor nanocrystals: synthesis and properties of InAs quantum rods. *Faraday Discuss* **2004**, *125*, 23-38, DOI: 10.1039/B302898D.

[36] Bera, S.; Ghosh, S.; Basu, R. N., Fabrication of

Bi_2S_3/ZnO Heterostructures: An Excellent photocatalyst for visible-light-driven hydrogen generation and photoelectrochemical properties, *New J. Chem*. **2018**, *42*, 541-554, DOI: 10.1039/ C7NJ03424E.

[37] Jayaprakash, G. K.; Kumara Swamy, B. E.; Casillasc, N.; Flores-Moreno, R., Analytical fukui and cyclic voltammetric studies on ferrocene modied carbon electrodes and eect of Triton X-100 by immobilization method, *Electrochim. Acta* **2017**, *258*, 1025-1034, DOI: 10.1016/j.electacta.2017.11.154.

[38] Jayaprakash, G. K.; Kumara Swamy, B. E.; Sánchez, J. P. M.; Li, X.; Sharma, S. C.; Lee, Sh., Electrochemical and quantum chemical studies of cetylpyridinium bromide modified carbon electrode interface for sensor applications, *J. Mol. Liq*. **2020**, *315*, 113719, DOI: 10.1016/j.molliq.2020.113719.